Solar Energy Conversion using a Broad Band Coherent Concentrator with Antenna-Coupled Rectifiers

P. Bodan[*], J. Apostolos[*], W. Mouyos[*], B. McMahon[*], P. Gili*, M. Feng[**]

[*]AMI Research & Development, LLC, Merrimack, NH, pbodan@ami-rd.com
[**]University of Illinois, Urbana, IL mfeng@illinois.edu

ABSTRACT

Through an internally funded research and development program, AMI Research and Development (AMI) has designed and developed a low profile, one-dimensional, solar coherent concentrator, intended for rectennas. A proof of concept prototype has been fabricated with an integrated photovoltaic array solar cell at the University of Illinois Urbana-Champaign (UIUC). Optical efficiency greater than 60% and an elevation field of view of 0.7 degrees has been modeled and confirmed with measurements. This device enables Antenna-Coupled Rectennas (ACR) to exceed one-sun solar performance efficiencies and provides a spectral splitting architecture to further enhance the efficiencies. We present the benefits of this device, prototype performance, and intended continued development of the ACRs.

Keywords: optical rectenna, antenna-coupled detectors, solar concentrator, coherent, metal-insulator-metal diode

1 INTRODUCTION

Although there has been incremental improvement in the efficiency of solar cells over the last decade, the cost per watt of installed solar energy systems has not crossed the threshold needed to attract consumers to use solar energy as a cost effective alternative to fossil fuels. Even with the declining cost of silicon and the near theoretical performance of multi-junction photovoltaic cells, the production cell efficiency needed to allow the dollars per watt threshold to be crossed is likely to be greater than 50%.

Antenna-coupled rectifiers are attractive for solar conversion because they can be made from much cheaper materials than semiconductor devices and they have theoretical efficiencies that approach the thermodynamic limit [1]. Additionally, studies have concluded that these devices, similar to semiconductor devices, can improve their efficiency under concentration and spectral splitting [1]. Refractive solar concentrators exist today, but none small enough to provide a coherent signal to an ACR. The size must be commensurate with the spatial coherence of the sun which is approximately 38μm in the linear dimension [2]. To further the viability of rectennas, we have developed a coherent concentrator that allows the use of inexpensive materials for conversion, provides a concentrated coherent signal to rectennas embedded in a waveguide to reduce the lossy metal antenna area required for rectennas, while residing in an architecture that facilitates spectral splitting.

Metal-insulator-metal (MIM) tunnel junctions are typically used as the rectifying element as they can be made an inherent part of the antenna during fabrication, and reside at the feed point of the antenna. Given the early state of MIM development, we have proven the concept of our design with a single junction GaAs photovoltaic cell and plan to confirm an extended bandwidth by using a multi-junction cell.

2 DESIGN CONCEPT

2.1 Coherent concentrator

The design of the coherent optical concentrator is based on antenna array principals, whereby a wedge prism serves as a continuous phased array coupler to a waveguide. The light at the base of the prism gets funneled through a narrow gap via evanescent wave coupling into a waveguide when the propagation constant across the boundary is matched in the axial direction of the waveguide. The result is phase coherent concentration in the waveguide. Input angular dependence, coupling of the evanescent field from the prism to the waveguide, and gap dependent theoretical monochromatic efficiencies up to 96% have been previously described in detail [3]. Using this coupling mechanism as a spectrally broadband, full-aperture, coherent, light concentrator is unique in functionality as well as application as detailed in patent numbers 8,437,082 and 8,422,111.

A physical block diagram of the AMI solar cell design is shown in Figure 1. It consists of the wedge prism aperture, a coupling gap, a broad band waveguide and an integrated photovoltaic array. Dimensions shown are commensurate with the spatial coherence of the sun and can be scaled for non-coherent applications. Peak efficiency across the solar spectrum is obtained from the optimization of three (3) key interdependent design parameters: 1) the gap thickness, 2) the waveguide effective dispersion, and 3) the coupling length to the photovoltaic cell. Design optimization was

done using both ANSYS HFSS and Optiwave FDTD, as well as internally developed Matlab design analysis tools.

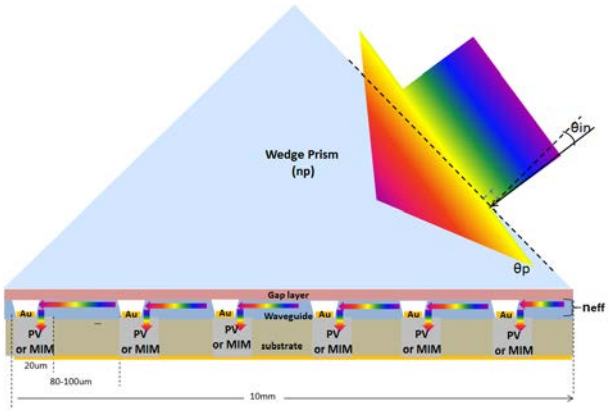

Figure 1 – Physical block diagram of Coherent Concentrator Array Cell

Broadband concentration is achieved by designing a waveguide that minimizes the angular variation across the solar spectrum for a given prism dispersion according to Equation 1. Here, the peak efficiency input angle is θ_{in}, θ_p is the prism angle, n_p is the prism index, and n_{eff} is the effective index of the waveguide. All parameters except θ_p are a function of wavelength. In operation, the device would use a single axis or micro tracker to maintain this angle.

$$\theta_{in}=\arcsin\{n_p*\sin[\theta_p-\arcsin(n_{eff}/n_p)]\} \quad (1)$$

Another aspect of the design is the integration of a total internal reflection (TIR) mirror in the waveguide. This reduces the concentrated flux area to less than a few micrometers, optimizes the concentration and optical throughput, and facilitates the vertical frequency selective antenna coupled MIMs as will be described later.

2.2 Frequency selective antenna-coupled rectifiers

Theoretical studies have concluded that an ideal ACR can convert broad band solar energy at up to 44% efficiency, while monochromatic light can be converted at up to 100% efficiency [1]. Therefore, analogous to obtaining higher efficiencies with multiple bandgaps for semiconductor devices, ACR conversion efficiency can be improved by spectrally splitting the solar energy for conversion with frequency selective antennas and optimizing the diode load for each ACR type. The vertical arrangement of frequency selective antenna coupled MIMs in place of the PVs in Figure 1 architecture accomplishes this. We utilize a bowtie antenna design for its broadband properties, simple MIM integration, and ease of fabrication.

The effective aperture, receive efficiency, resonant wavelength and bandwidth of the antenna are controlled by geometry. For energy harvesting, these performance parameters are traded off to optimize a high AC to DC rectification efficiency. Figure 2 shows the output of an HFSS FEM model of three (3) bowtie designs, each tuned for a different wavelength and spaced spectrally to contiguously cover the solar bandwidth with greater than 80% normalized efficiency.

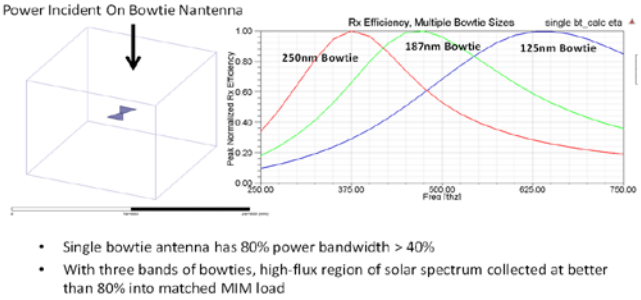

Figure 2 – Example of 3 bowtie antennas covering majority of solar spectrum

Since the effective area of a single bowtie is expected to be less than the spot size of the beam exiting the waveguide, antenna rectifying elements are arrayed both laterally and vertically as shown in Figure 3. Energy that is not converted is either lost due to resistive losses in the material, scattered, or continues to propagate past the rectenna.

Figure 3 shows an FEM model of the stacked, banded bowtie rectenna approach. It is similar to a log periodic array, wherein out of band energy continues through the region of higher frequency tuned dipoles and is eventually collected at the tuned, in-band dipoles. The model shows this occurring at optical frequencies as well, and indicates that two (2) or three (3) layers of stacked bowties reduce the incident power field by approximately 8 dB in the band of operation, while little power is lost to out of band or in-band energy scattering from the rectenna structures. Providing a concentrated coherent input to the stack allows minimizing the lateral number of bowties, and hence material losses, and provides the potential for increased non-linearity during rectification for higher efficiency.

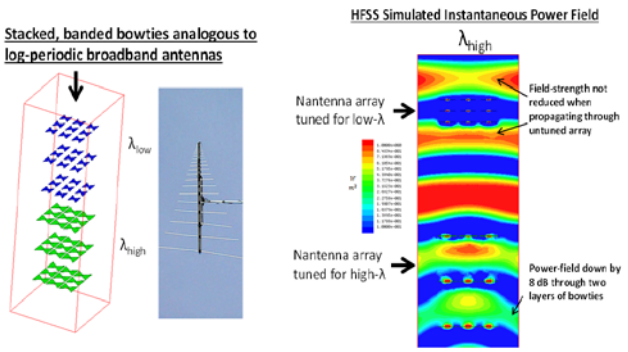

Figure 3 – Spectral splitting using filtering properties of antennas

2.3 Rectenna end-to-end SPICE model

An LTSPICE model has been created to validate system level conversion efficiency predictions and to determine optimum circuit component values. Results and conclusions obtained are valid to the extent that quantum effects can be included in the model for the MIM diode. A nonlinear voltage controlled current source is implemented in the model and power calculators are included to measure the average instantaneous DC power delivered to the load and AC power available from the antenna as shown in Figure 4.

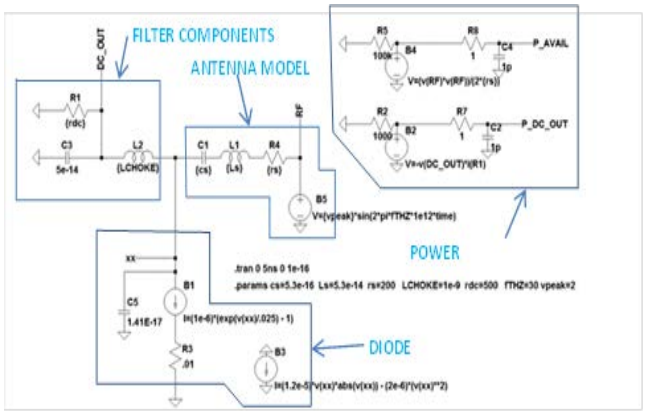

Figure 4 – LTSPICE schematic for rectenna simulation

3 FABRICATION

A prototype of the concentrator was fabricated at UIUC and integrated with a PV device for proof of concept testing. Figure 5 shows the 0.5 inch x 0.5 inch unit cell. Since the 20μm photovoltaic cells depicted in Figure 1 were not available, the prototype was fabricated from a GaAs wafer that was the length of the array.

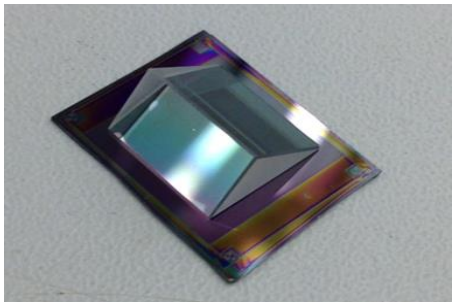

Figure 5 – AMI solar concentrator prototype unit cell

3.1 Array fabrication

A constant thickness layer of MgF_2 is used for the evanescent coupling layer at the base of the prism to simplify fabrication and provide more reliable geometry to test the accuracy of the numerical models. In order to have the most control of the effective index of the waveguide to accomplish dispersion matching according to equation 1, we have designed a multilayer SiON structure. The waveguide layers are deposited via PECVD on a GaAs wafer and the TIR mirrors were fabricated using wet etching. During the fabrication process of the multi-index layered SiON wideband waveguide, SiH_4, N_2O, and NH_4OH were used for reaction gas in PECVD thin film deposition, and NH_4OH was varied to achieve the different compositions of SiON. All the SiON thin films were characterized by spectroscopic ellipsometry to determine the thickness and the refractive index. A scanning electron microscope (SEM) image of the cell is shown in Figure 6.

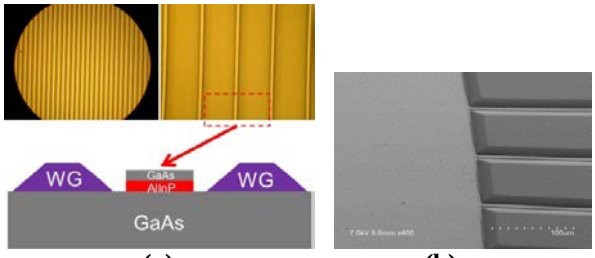

(a) **(b)**

Figure 6 – a) SEM image and cross-sectional diagram of etched solar cell, b) SEM image showing 45° angle etch

3.2 Antenna-coupled MIM Diode Fabrication

In addition to prototyping a unit cell, we have begun a three (3) stage development process at UIUC to fabricate ACRs and integrate them into the concentrator. Designs are starting at an operating wavelength of 10.6 μm, and progressing to 1550 nm, and eventually visible light. Our first integrated Nickel-Nickel Oxide-Nickel metal-insulator-metal (MIM) rectifier defined using electron beam lithography and fabricated with shadow evaporation metal deposition is shown in Figure 7.

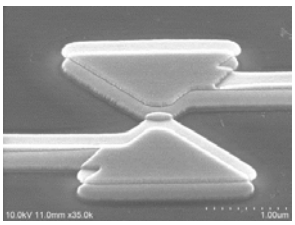

Figure 7 – Bowtie antenna and Ni-NiO-Ni MIM diode

Two (2) critical factors in producing reliable MIMs are first layer metal flatness and oxide thickness control. These aspects are being examined in detail using a larger scale format before being implemented on smaller devices.

4 RESULTS

The unit cell in Figure 5 has been tested in an indoor laboratory using lasers as well as outdoors with sun illumination. Indoor testing has been accomplished using

four (4) lasers at wavelengths of 405 nm, 532 nm, 632 nm and 808 nm. The limitation to 808 nm is due to the GaAs PV used in this prototype. The indoor angular pattern scan results are shown in Figure 8 and the outdoor results in Figure 9.

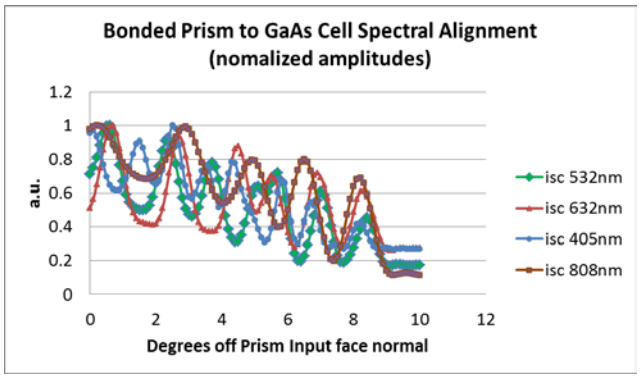

Figure 8 – Indoor angular pattern scan of 1J unit cell

To obtain the 'antenna pattern' of the device, the unit cell's short circuit current response to angularly scanned collimated monochromatic light was measured using the four (4) lasers. Data are normalized due to various laser powers being used. The fundamental mode (m=0) of the waveguide is the peak current at the largest angle off the prism normal (0 degrees). Other higher order modes are present as well, but they are not aligned over the spectrum. As shown on the graph, the angular peak locations of the fundamental mode are aligned to within 0.3 degrees across the spectrum at an approximate angle of 8.3 degrees. Without dispersion compensation, the angular variation would be approximately 5.0 degrees, and the device would not have good efficiency across the solar spectrum. Confirmation of mode alignment at 980 nm and 1310 nm for the waveguide design was accomplished on another device. The residual current between peaks of other modes is due to light not being in a guided mode at those angles and the presence of the extended PV beneath the waveguide cladding. This is specific to the process used for proof of concept and should not be present with smaller PVs or MIM devices.

The optical efficiency of the device was measured at the aligned fundamental mode by comparing the short circuit current of a device from the same wafer without a prism to another cell with a prism. The results for the four (4) lasers were 29%, 30%, 42% and 61%, respectively. This is in close agreement with the Optiwave modeled results to within 10%. Measurements include the non-current producing TIR etched area which has not been minimized during proof of concept, and is currently approximately 15% of the overall cell area. A reduction in the size of this area is expected in the future. These indoor results confirm the simulations. It is expected that an aggregate full spectrum solar weighted optical efficiency of greater than 65% is achievable at the angle of the fundamental mode.

A walk-through preliminary angular scan of the unit cell taken on a clear day is shown in Figure 9. A short circuit current density of 25 mA/cm^2 of the cell was measured before prism bonding. The short circuit current density of the unit cell after prism bonding at the fundamental mode was 14.8 mA/cm^2. This is evident at the peak at -4 degrees in Figure 9. This is approximately a 56% optical throughput up to the bandgap of GaAs (850nm), including the trapezoidal etched area for contacts and TIR mirror. It is expected that these data have up to 20% error due to flux impingement area measurements, flux uncertainty, stray light and other factors. However, these data look very promising and do confirm proof of concept of the device. Optiwave simuilations show the throughput above 808nm to be in excess of 61%. Several design improvements are in process to provide better efficiency.

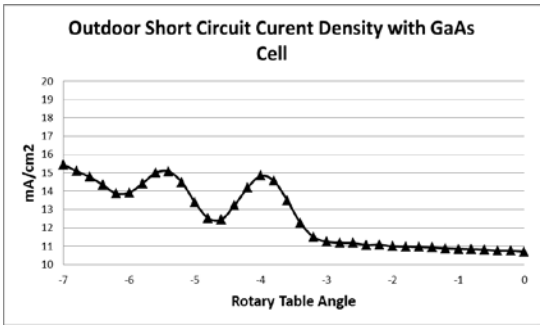

Figure 9 – Outdoor angular pattern scan of 1J unit cell

5 CONCLUSION

Given the recent advancements of nanotechnology, we see the increased possibility for direct electromagnetic conversion of solar energy via rectennas. To advance their viability we have completed the preliminary design of a coherent solar concentrator. The design provides a low concentration (<100x) open architecture for vertically stacked frequency selective rectennas, and could also provide a low profile concentrator for semiconductor cells. Simulation results and supporting lab measurements confirm achievable optical efficiencies greater than 65%. Future efforts are planned to incorporate 1550nm bowtie coupled MIM diodes for full concentrated EM conversion.

REFERENCES

[1] S. Joshi and G. Moddel, Applied Physics Letters 102, 083901 (2013).
[2] H. Mashaal, J.M. Gordon, Opt. Lett. 36, pp.900-902, 2011.
[3] R. Ulrich, JOSA, Vol. 60, No. 10, pp.1337-1350 (1970).